

Large- q neutron inclusive-scattering data from liquid ^4He

A. S. Rinat and M. F. Taragin

Department of Particle Physics, Weizmann Institute of Science, Rehovot 76100, Israel

F. Mazzanti and A. Polls

Department d'Estructura e Constituents de la Materia, Diagonal 645, Universitat de Barcelona, E-08028 Barcelona, Spain

(Received 10 June 1997)

We report dynamical calculations for large- q structure functions of liquid ^4He at $T=1.6$ and 2.3 K and compare those with recent MARI data. We extend those calculations far beyond the experimental range $q \leq 29 \text{ \AA}^{-1}$ in order to study the approach of the response to its asymptotic limit for a system with interactions having a strong short-range repulsion. We find only small deviations from theoretical $1/q$ behavior, valid for smooth V . We repeat an extraction by Glyde *et al.* of cumulant coefficients from data which are invariably very well reproduced. We argue that fits determine the single atom momentum distribution, but express doubt as to the extraction of meaningful final state interaction parameters.

[S0163-1829(98)02709-X]

I. INTRODUCTION

In the following we discuss different aspects of the response of liquid ^4He to density fluctuations which is measured in large- q neutron inclusive scattering against liquid ^4He . The linear response is a function of two parameters q and ω , which in the scattering experiment are the momentum and energy transferred from the projectile to the target. For medium and large q those responses contain information on the target, such as the momentum distribution of the constituents and prescribed manifestations of their interaction which are commonly known as final-state interactions (FSI). The state of the art of the field and extensive references have recently been reviewed by Glyde.¹

First we report predictions which are compared with most recent data. Next, we compute the response for $q \leq 300 \text{ \AA}^{-1}$ in order to study how FSI effects vanish for large q . In the end we present results of a model-independent cumulant analysis of data in order to extract the single-atom momentum distribution and interaction parameters.

Recent precision data for temperatures below and above the transition temperature T_c have been taken at the Rutherford ISIS facility by means of the MARI spectrometer. Those by Andersen *et al.* span neutron momentum transfers $3 \leq q(\text{\AA}^{-1}) \leq 10$ for $T=1.42$ K and $3 \leq q(\text{\AA}^{-1}) \leq 17$ for $T=2.5$ K,² while Azuah's measurements covered $10 \leq q(\text{\AA}^{-1}) \leq 29$ for $T=1.6$ and 2.3 .³ The present results expand in scope previous information taken a few years ago at the IPNS facility at Argonne for $q \leq 23.1 \text{ \AA}^{-1}$.⁴

To our knowledge no *ab initio* calculations of the MARI data have previously been performed. Such calculations require as input the atom-atom interaction and ground-state information, which for the above q regime are primarily the single-atom momentum distribution $n(p)$ and the semidiagonal two-particle density matrix.

Using variations of much the same theory, predictions have been made before for medium- q , as well as for the higher- q Argonne data.⁵⁻⁹ The above-mentioned MARI data

have recently been approached in an entirely different fashion with the purpose of determining in a model-independent way the dominant coefficients in the cumulant expansions of the asymptotic and FSI parts of the response.^{10,11,12} Good fits to the data were obtained, but those have little in common with dynamic calculations. The latter use as *input* $n(p)$, additional ground-state information, and V whereas, ideally, $n(p)$ and properties of V are *extracted* from cumulant fits.

As a major result of the above analysis, Glyde *et al.* report the reconstruction of the single-atom momentum distribution $n(p)$ in good agreement with accurate theoretical predictions.^{13,14} However, a less satisfactory feature is the extracted dominant FSI cumulant coefficient which, dependent on the analysis, is reported to be less than 0.65 times the calculated value. One then wonders whether the apparent partial fit may have consequences on the precision of the reconstructed $n(p)$. We shall demonstrate that in spite of the misfit of FSI parameters, their minor role hardly affects the stability of the extracted $n(p)$, at least for $T > T_c$ when the condensate fraction is absent.

The following program emerges from the above observations. In Sec. II we outline an approach to high- q responses. In Sec. III we report computations of the high- q measurements using the MARI spectrometer and compare those predictions with the data. In addition we interpret responses computed out to very high $q \leq 300 \text{ \AA}^{-1}$. The results enable the study of the approach of the response to its asymptotic limit for systems with a strong short-range repulsion in the interaction between the constituents. In Sec. IV we present fits for cumulant parameters for $T=2.3$ K and compare those with similar results by Glyde *et al.*¹⁰⁻¹² We discuss the discrepancy between the calculated and the extracted FSI parameters and attribute it to the truncation of the cumulant series. In the conclusion we estimate that both experimental and theoretical studies of the response of liquid ^4He at high q may have reached a degree of sophistication, beyond which there is little prospect to gain new information.

II. DESCRIPTIONS OF THE LINEAR RESPONSE FOR HIGH Q

Consider for infinitely extended liquid ${}^4\text{He}$ the response per atom in the form

$$S(q, \omega) = A^{-1} (2\pi)^{-1} \int_{-\infty}^{\infty} dt e^{i\omega t} \langle 0 | \rho_q^\dagger(t) \rho_q(0) | 0 \rangle, \quad (1)$$

$$\phi(q, y) = (q/M) S(q, \omega),$$

with M the mass of a ${}^4\text{He}$ atom. $\rho_q(t)$ above is the density operator

$$\rho_q(t) = e^{-iHt} \rho_q(0) e^{iHt}, \quad (2)$$

$$\rho_q(0) = \sum_j e^{iqr_j(0)}.$$

Strictly speaking, the symbol $\langle 0 | \dots | 0 \rangle$ should stand for a canonical average at given T , but we shall use instead the ground state in conjunction with T -dependent quantities.

In the last line of Eq. (1) we introduce the reduced response $\phi(q, y)$ with the energy loss ω , replaced by an alternative kinematic variable $y = y(q, \omega)$ (Refs. 15,16)

$$y = \frac{M}{q} \left(\omega - \frac{q^2}{2M} \right). \quad (3)$$

Upon substitution of Eq. (2) into Eq. (1) one generates two components of the response. In the incoherent part, one tracks the same particle when propagating in the medium, while in the coherent part one transfers momentum and energy to a particle distinct from the struck one. For $q \gtrsim 8 \text{ \AA}^{-1}$ the response is dominated by the incoherent part and the coherent part can be safely disregarded.

For the description of the large- q response we shall exploit the theory of Gersch, Rodriguez, and Smith (GRS) for smooth interactions V which leads to the following expansion for the reduced response in inverse powers of q or of the recoil velocity $v_q = q/M$ (Ref. 15) (we use units $\hbar = c = 1$ causing all quantities to have dimensions of powers of \AA^{-1}):

$$\phi(q, y) = \sum_{n=0}^{\infty} \left(\frac{1}{v_q} \right)^n F_n(y), \quad (4a)$$

$$F_0(y) = \lim_{q \rightarrow \infty} \phi(q, y) = (4\pi^2)^{-1} \int_{|y|}^{\infty} dp p n(p), \quad (4b)$$

$$\begin{aligned} \frac{1}{v_q} F_1(y) &= i(2\pi\rho)^{-1} \int_{-\infty}^{\infty} ds e^{iys} \\ &\times \int dr \rho_2(\mathbf{r}, 0; \mathbf{r} - s\hat{q}, 0) \tilde{\chi}(q; \mathbf{r}, s), \end{aligned} \quad (4c)$$

$$\begin{aligned} \tilde{\chi}(q, \mathbf{r}, s) &= -\frac{1}{v_q} \left[\int_0^s ds' V(\mathbf{r} - s'\hat{q}) \right. \\ &\left. - sV(\mathbf{r} - s\hat{q}) \right] \dots, \text{ etc.} \end{aligned} \quad (4d)$$

The function $\tilde{\chi}$ in Eq. (4d) resembles an eikonal phase. It differs from it because the integration limits on the line integral over the first component of V are not $(-\infty, \infty)$, as is appropriate for on-shell scattering. The finite limits correspond to off-shell scattering described in the coordinate representation. Moreover a second interaction is implicit in Eq. (4d). In the following we shall allude to the total expression (4d) as the generalized eikonal phase.

We recall the interpretation of the lowest-order terms. For sufficiently large momentum transfer q , an atom with initial momentum p recoils with $p' = |p + q| \approx q \gg \langle p^2 \rangle^{1/2}$, which is larger than the average momentum of an atom in the medium and is moreover in excess of any inverse length in the system. The recoiling atom moves therefore too fast to be affected by atom-atom collisions and the response is the asymptotic limit $F_0(y)$ for $q, \omega \rightarrow \infty$ at fixed y . Equation (4b) shows its expression in terms of the single-atom momentum distribution, normalized as $\int dp / (2\pi)^3 n(p) = 1$.

Although the GRS theory is not a perturbation theory in the interaction V , the second term in the series (4a), linear in V , is entirely due to binary collisions (BC) between the hit and any other atom. It accounts for the dominant FSI collecting all contributions $\propto 1/q$. This is achieved at the price of introducing the semidiagonal two-particle density matrix ρ_2 in Eq. (4c).

In another publication Gersch and Rodriguez suggested an alternative representation for the reduced response¹⁷

$$\begin{aligned} \phi(q, y) &= \int dy' F_0(y - y') R(q, y') \\ &= \int \frac{dp}{(2\pi)^3} n(p) R(q, y - p_z), \end{aligned} \quad (5a)$$

$$\begin{aligned} \tilde{\mathcal{F}}(q, s) &= \int_{-\infty}^{\infty} dy e^{-iys} \phi(q, y) = \sum_n \left(\frac{1}{v_q} \right)^n \tilde{F}_n(s) \\ &= \tilde{F}_0(s) \tilde{R}(q, s) \equiv \tilde{F}_0(s) \exp[\tilde{\Omega}(q, s)]. \end{aligned} \quad (5b)$$

In Eq. (5a) the response is written as a convolution of its asymptotic limit and a FSI factor $R(q, y)$. It is frequently convenient to use Fourier transforms $\tilde{F}_i(q, s), \tilde{R}(q, s) \dots$. In particular for the first two terms in Eq. (5b) one has [cf. Eqs. (4b) and (4c)]

$$\tilde{F}_0(s) = \frac{\rho_1(s, 0)}{\rho} = \int \frac{dp}{(2\pi)^3} e^{-ip\hat{q}s} n(p), \quad (6a)$$

$$\frac{1}{v_q} \tilde{F}_1(s) = \frac{i}{\rho} \int dr \rho_2(\mathbf{r} - s\hat{q}, 0; \mathbf{r}, 0) \tilde{\chi}(q; \mathbf{r}, s), \quad (6b)$$

with $\rho_1(s, 0) = \rho_1(\mathbf{r} - s\hat{q}, \mathbf{r})$, the single-atom density matrix and $\rho = \rho_1(\mathbf{r}, \mathbf{r})$, the number density.

We shall restrict ourselves below to various descriptions of FSI due to BC, starting from the corresponding cumulant form (5b) and using Eq. (6a) (Ref. 17)

$$\bar{\phi}(q,s) = \frac{\rho_1(s,0)}{\rho} \bar{R}_2(q,s) = \frac{\rho_1(s,0)}{\rho} \exp[\bar{\Omega}_2(q,s)],$$

$$\bar{\Omega}_2(q,s) = i\rho \int d\mathbf{r} \zeta_2(\mathbf{r},s) \omega_2(q,\mathbf{r},s), \quad (7)$$

where $\bar{R}_2(q,s)$ and $\bar{\Omega}_2(q,s)$ are the BC approximation to the corresponding quantities defined in Eqs. (5a) and (5b). ζ_2 above is defined by

$$\zeta_2(\mathbf{r},s) = \frac{\rho_2(\mathbf{r}-s\hat{\mathbf{q}};0;\mathbf{r},0)}{\rho\rho_1(s,0)}, \quad (8a)$$

$$\zeta_2(\mathbf{r},0) = g_2(\mathbf{r}) \quad (8b)$$

with g_2 the pair-distribution function.

Equation (7) is the most general cumulant form in the BC approximation for the FSI phase $\bar{\Omega}_2(q,s) = \ln[\bar{R}_2(q,s)]$, and distinguishes through ω_2 between different dynamical approaches. For instance, for smooth interactions V , which would allow for an expansion of the exponential in Eq. (7), comparison of Eqs. (7), (5b), and (4d) shows ω_2 to be the generalized eikonal phase

$$\omega_{2,V}(q,\mathbf{r},s) = \tilde{\chi}(q,\mathbf{r},s). \quad (9)$$

For interactions with a strong short-range repulsion, the line integral over V in the (off-shell) phase (4d) which enters the dominant BC FSI contribution $\bar{F}_1(s)$, Eq. (6b), may produce large and even divergent integrals. The standard method to tackle those difficulties is by partial summation of selected higher-order terms

$$i\omega_{2,V} \rightarrow i\omega_{2,t} = e^{i\tilde{\chi}} - 1, \quad (10)$$

which amounts to replacing the bare V by a q -dependent effective interaction $V \rightarrow V_{\text{eff}}(q) = \tilde{t}(q)$, the latter being the off-shell t matrix, in turn generated by V . Moreover the propagation in between collisions is described in the eikonal approximation.^{7,18}

In an alternative regularization for an atom-atom interaction with a strong short-range repulsion, one replaces the generalized eikonal phase (4d) by a semiclassical approximation^{19,20}

$$\omega_{2,sc}(q,\mathbf{r},s) = iq \int_0^s ds' \left[\sqrt{1 - \frac{2m}{q^2} V(\mathbf{r}-s'\hat{\mathbf{q}})} - \sqrt{1 - \frac{2m}{q^2} V(\mathbf{r}-s\hat{\mathbf{q}})} \right]. \quad (11)$$

For $(2m/q^2)V \ll 1$, $\omega_{2,sc}$ coincides with $\omega_{2,V}$, Eq. (9). However, in classically forbidden regions $(2m/q^2)V > 1$, $\omega_{2,sc}$ describes damping, as the dominant imaginary part of $V_{\text{eff}}(q)$ in (10) is expected to do. This will be borne out by calculations.

Whereas $\omega_{2,V}$ is strictly proportional to $1/q$, this is no more the case for $\omega_{2,t}$ after the replacement $V \rightarrow V_{\text{eff}}(q)$. The above manifestly introduces q dependence in coefficients of the GRS series (4a),(5b) and in particular in the BC approximation. Taking the latter in the cumulant form (7) adds to the

blurring of the original $1/q$ dependence. This raises the question how the response approaches its asymptotic limit.

We start with a theoretical analysis of the first cause of additional q dependence and focus on ^4He - ^4He scattering for high lab momenta q . The latter is of a distinctly diffractive nature, typical for interactions with a strong, short-range repulsion. For those, the dominant imaginary part of the on-shell scattering amplitude $t(q) \approx \text{Im}f(q) \propto iq\sigma_q^{\text{tot}}$, where the total ^4He - ^4He cross section σ_q varies much slower than q itself.⁶

Without entering into details, we state that the off-shell $\tilde{t} = V_{\text{eff}}$ in ω_2 , Eq. (7), can approximately be related to the on-shell scattering amplitude for elastic scattering. (See Ref. 21 for a more extensive treatment of the parallel discussion for atomic nuclei). It can then be shown that the rigorous proportionality of the dominant BC FSI phase $\bar{\Omega}_{2,V} \propto 1/q$ for a smooth, bare V still holds approximately for $\bar{\Omega}_{2,t}$.

Additional q dependence is due to the use of the cumulant representation (7) but it will be small to the extent that FSI are. In conclusion, the reduced response described by Eqs. (5) and (7) is expected to approximately preserve the $1/q$ signature of the dominant binary collision contribution. We shall return below to a numerical confirmation.

III. DYNAMICAL CALCULATIONS OF SELECTED MARI ^4He DATA

We first mention and discuss the input elements which suffice for the BC approximation in any of the forms described in Sec. II.

(a) The atom-atom interaction V_{Aziz} .²²

(b) The single-atom momentum distribution $n(p,T)$:

$$n(p;T) = (2\pi)^3 \delta(\mathbf{p})n_0(T) + [1 - n_0(T)]n^{\text{NO}}(p;T),$$

$$\frac{\rho_1(s,0;T)}{\rho} = n_0(T) + [1 - n_0(T)] \frac{\rho_1^{\text{NO}}(s,0;T)}{\rho}. \quad (12)$$

$n_0(T \leq T_c)$ is the fraction of atoms in the condensed state,²³ $n^{\text{NO}}(p;T)$ and $\rho_1^{\text{NO}}(s,0;T)/\rho$ above are, respectively, the momentum distribution of the normal (uncondensed) atoms and its Fourier transform. Path integral Monte Carlo (PIMC) calculations have shown moderate T dependence of $n^{\text{NO}}(p;T)$ for $T \leq 4$ K.^{13,25}

(c) The least accessible ground-state property required in the BC approximation is the semidiagonal, two-body density matrix which weights the dominant BC FSI terms in Eqs. (4c) or (5b). Calculations based on a variationally determined ground-state wave function in the hypernetted chain (HNC) formalism produce for ζ_2 , Eq. (8) (Refs. 26 and 9):

$$\zeta_2^{\text{HNC}}(\mathbf{r},s;\xi) = g_{wd}(\mathbf{r})g_{wd}(|\mathbf{r}-s\hat{\mathbf{q}}|)\exp[A(\mathbf{r},s)] \\ \approx g_{wd}(\mathbf{r})g_{wd}(|\mathbf{r}-s\hat{\mathbf{q}}|)\exp[\xi A_4(\mathbf{r},s)],$$

$$A_4(\mathbf{r},s) = \rho \int d\mathbf{r}' [g_{wd}(|\mathbf{r}'-s\hat{\mathbf{q}}|) - 1][g_{wd}(\mathbf{r}') - 1] \\ \times [g(|\mathbf{r}'-\mathbf{r}|) - 1]. \quad (13)$$

$g_{wd}(\mathbf{r})$ is an auxiliary function related to what in HNC formalism is called a form factor.²⁶ The function $A(\mathbf{r},s)$ for-

mally adds all so-called Abe diagrams and is approximated in Eq. (13) by the four-body Abe diagram $A_4(\mathbf{r}, s)$, using in addition a scaling parameter ξ .^{9,27}

Far less sophisticated and simpler is the GRS approximation¹⁵

$$\zeta_2^{\text{GRS}}(\mathbf{r}, s) = \sqrt{g(\mathbf{r})g(\mathbf{r}-s\hat{\mathbf{q}})}, \quad (14)$$

which interpolates ζ_2 between $s=0$ and the Hartree limit for large s .¹⁵

Both options have drawbacks and fail for instance the extended unitarity test

$$\int d\mathbf{r} \rho_2(\mathbf{r}-s\hat{\mathbf{q}}; 0; \mathbf{r}, 0) = (A-1)\rho_1(s, 0), \quad (15)$$

which can be written as

$$\Xi(s) = \rho \int d\mathbf{r} [1 - \zeta_2(\mathbf{r}; s)] = 1. \quad (16)$$

Using a typical pair-distribution function $g(r)$, $\Xi(s)$ above computed with ζ_2^{GRS} , Eq. (14), produces values up to 1.7 for $s=2.0$ instead of the exact value 1.0, independent of s .²⁸ In the HNC case, approximations involved in the evaluation of the Abe terms (13) are responsible for similar deviations of $\Xi(s)$ from 1. The violation of condition (16) is intrinsic in the GRS approximation (14), no matter what $g(r)$ is used.

Another important constraint is the fact that the diagonal two-body density matrix should coincide with the pair-distribution function: $\zeta_2(\mathbf{r}, 0) = g(r)$, Eq. (8b). While the GRS approximation fulfills that condition by construction, a full evaluation of the Abe terms is necessary in the HNC formalism. Demanding the boundary value condition to be fulfilled in the mean, one determines the so-called scaling parameter ξ by minimizing the following quantity:

$$\sigma(\xi) = \int d\mathbf{r} |\zeta^{\text{HNC}}(\mathbf{r}, 0; \xi) - g(r)|^2.$$

A particular choice of ζ_2 presumably matters for medium q , but for increasing $q \gtrsim 20 \text{ \AA}^{-1}$ FSI contributions decrease in importance relative to the asymptotic response. A few-percent spread, due to uncertainty in the choice of ζ_2 , in already small FSI terms will go unnoticed. We thus opted for expression (14) which is numerically much easier to handle than Eq. (13).

(d) Finally, for a comparison of actual data with predictions the latter have to be folded into the experimental resolution function (ER) $E(q, y; T)$ of the instrument. The $E(q, y; T)$ corresponding to the $q \gtrsim 20 \text{ \AA}^{-1}$ MARI data are given in Azuah's thesis³ and have been fitted to the sum of two off-center gaussians. No ER, pertinent to lower q 's were available to us, thus precluding an analysis for $q \leq 20 \text{ \AA}^{-1}$.

Until this point we did not specify the T dependence of the theoretical responses. In fact one ought to employ quantities computed for given T . Actually, there exist experimental data²⁹ and also PIMC studies^{13,25} on the T dependence of the pair-distribution function $g(r, T)$. However, in view of the above arguments we shall use the one for $T=0$. By the same token ζ_2 , Eq. (14), and consequently FSI effects will be independent of T . This leaves the single-particle density

matrices, or equivalently the momentum distributions as the only T -dependent quantities in the present analysis. We took $n_0(T=1.6 \text{ K})=0.087$ and $\rho_1^{\text{NO}}(0, s; T=1.6 \text{ K}) = \rho_1(0, s; T=2.3 \text{ K})$ from calculations for $T=1.54$ and 2.5 K .^{13,25}

The expression for the predicted response is therefore

$$\phi(q, y; T \geq T_c) = \int \frac{d\mathbf{p}}{(2\pi)^3} n(\mathbf{p}; T) R(q, y - p_z), \quad (17)$$

$$\phi(q, y; T \leq T_c) = n_0(T) R(q, y) + [1 - n_0(T)]$$

$$\times \int \frac{d\mathbf{p}}{(2\pi)^3} n^{\text{NO}}(\mathbf{p}; T) R(q, y - p_z),$$

which in order to enable a comparison with data, has to be folded into ER

$$\begin{aligned} \phi_E(q, y; T) &= \int_{-\infty}^{\infty} dy' E(q, y - y'; T) \phi(q, y'; T) \\ &= (2\pi)^{-1} \int_{-\infty}^{\infty} ds e^{iys} \tilde{E}(q, s, T) \tilde{\phi}(q, s; T). \end{aligned} \quad (18)$$

For future reference we emphasize here that the FSI factor R is, from Eqs. (7) and (8), seen to be independent of the single-particle density matrix $\rho_1(s, 0)/\rho$. In particular for all but pure hard-core interactions

$$\lim_{q \rightarrow \infty} \tilde{R}(q, s) = 1. \quad (19)$$

We thus computed the reduced response $\phi_E(q, y; T)$, for the $q=21, 23, 25, 29 \text{ \AA}^{-1}$ sample out of the MARI data. In view of the steady decrease of FSI, this q range and steps seems to be sufficient for our study. We emphasize in particular the case $q=23 \text{ \AA}^{-1}$, considered because it is the largest q in the older Argonne data sets⁴ and for it we shall compare our results with others.

We start with a comparison of our predictions for $T=2.3 \text{ K}$ and the corresponding data³ [Figs. 1(a)–1(d)]. The overall agreement is very good. One notices that, whereas the central value for the theoretical response hardly changes for $21 \leq q(\text{\AA}^{-1}) \leq 29$, the data for the same, folded in the ER, $\phi_E(q, 0)$ show q dependence present in $E(q, y)$.

The agreement for $T=1.6 \text{ K}$ [see Figs. 2(a)–2(d)] is slightly worse. The slight staggering in the central region for $q=21 \text{ \AA}^{-1}$ is probably of instrumental origin, but contrary to the $T=2.3 \text{ K}$ case, differences in $E(q, y)$ for $q=21, 29 \text{ \AA}^{-1}$ do not explain the small discrepancies in their central regions. We recall that exactly the same input is used as for $T=2.3 \text{ K}$ and that the only extra parameter is the condensate fraction $n_0(T=1.6 \text{ K})$.

We now reach our second topic. In spite of the fact that no data exist for $q \gtrsim 29 \text{ \AA}^{-1}$, we have extended calculations up to $q=300 \text{ \AA}^{-1}$. The purpose of the exercise is to obtain *theoretical* information on the approach of the response to its asymptotic limit.

In Fig. 3(a) we present $\phi^{\text{even}}(q, y, T=2.3 \text{ K})$ which is the part of the response, even in y and computed in the BC approximation (7),(10). Even in the wings out to $y \approx 3.5 \text{ \AA}^{-1}$

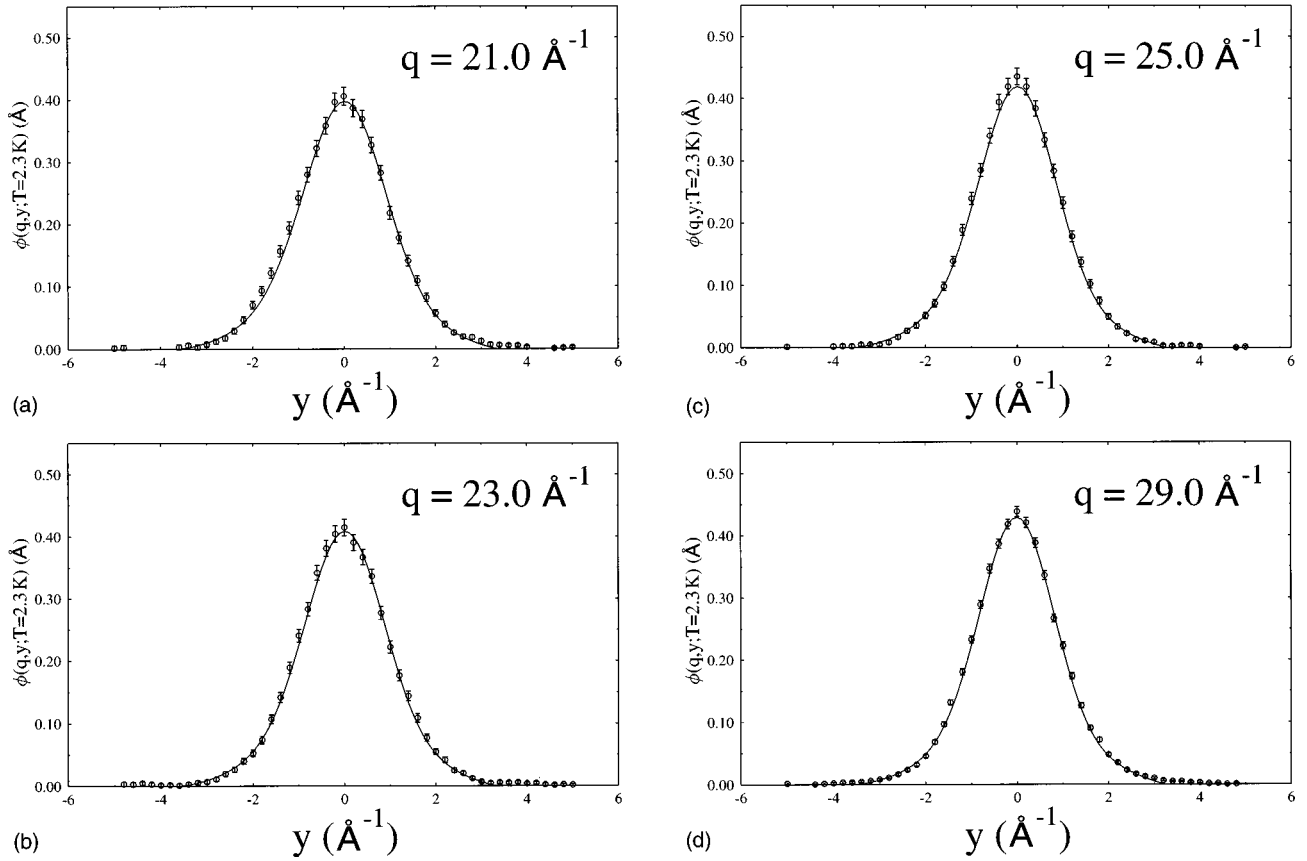


FIG. 1. (a)–(d) Predictions for the response (5),(7) of liquid ^4He at $T=2.3$ K for $q=21, 23, 25, 29$ \AA^{-1} from Eq. (7) using the ladder approximation (10) for binary collisions. Those results have been folded with the experimental resolutions from Azuah's thesis, which is also the source of data (Ref. 3).

those coincide within 1% among themselves and with the asymptotic response $F_0(y)$, Eq. (4b). The above appears hardly changed, when predictions for $20 \leq q(\text{\AA}^{-1}) \leq 29$ are included: only in the immediate neighborhood of $y=0$, is there a $\leq 2.5\%$ difference.

In Fig. 3(b) we show $q\phi^{\text{odd}}(q, y, T=2.3$ K), the part of the response which is odd in y , multiplied ϕ^{odd} by q . The latter is the signature of the dominant FS. Some residual q dependence is then apparent in Fig. 3(b) in the extrema as well as in the wings. However, the true measure for the size of FSI is the ratio $\phi^{\text{odd}}/\phi^{\text{even}}$ which is at most a few percent. The conclusion is clear: Neither the strong short-range repulsion in the atom-atom interaction which forces the use of $V_{\text{eff}}(q) = \tilde{t}(q)$, nor the effect of the cumulant representation, much changes the $1/q$ signature of the dominant FSI term in the GRS series (4a) for smooth V . The above agrees with our arguments in Sec. II and with our previous results.⁶

All reported predictions are based on the use of the t matrix, i.e., on Eq. (10). In Sec. II we also mentioned a semiclassical approximation (11) for FSI and found that, except for small s , there are considerable differences between the BC phases, calculated by means of Eqs. (11) and (10). Ultimately excellent agreement is obtained between the corresponding responses, computed with Eqs. (5) and (7). Clearly both the t -matrix and the semiclassical method accurately describe the binary collision phase in the salient region just inside the classically forbidden region. Contributions from deeper penetration distances are strongly suppressed.

We conclude this section by a discussion and comparison of predictions for $q=23$ \AA^{-1} by other authors. Since the various studies refer to different T and data have been taken at different instruments, the natural quantity to compare is the FSI factor $R(q, y)$ assumed to be T independent.

We start with predictions by Mazzanti *et al.*⁹ which are based on exactly the same BC approximation in the V_{eff} version (10), employing however the variationally derived ζ_2^{HNC} , Eq. (13). Next we mention Silver⁵ who used, what amounts to the cumulant form (7) with $\omega_2 \rightarrow \omega_{2,t}$ and $\zeta_2 \rightarrow g_2$, the pair-distribution function. In his hard-core perturbation theory he disregarded the second part of the total phase χ , Eq. (4d), which is only permissible for a *pure* hard-core interaction. However, Silver actually constructed the off-shell t matrix in Eq. (10), corresponding to the first part in Eq. (4d) from JWKB partial wave phase shifts for a realistic V , which in addition to strong short-range repulsion also included attractive components. Nevertheless, he neglected the second component in Eq. (4) which does not vanish when an attraction is present. We conclude with a path-integral method by Carraro and Koonin, who computed high- q FSI using a fixed scattering approximation for the entire system with a large, finite number of atoms.⁸ The method requires the parallel calculation of the ground-state wave function in order to construct the N -body density matrix, diagonal except for one particle, with N the number of atoms in the sample and which averages the response for fixed scatterers.

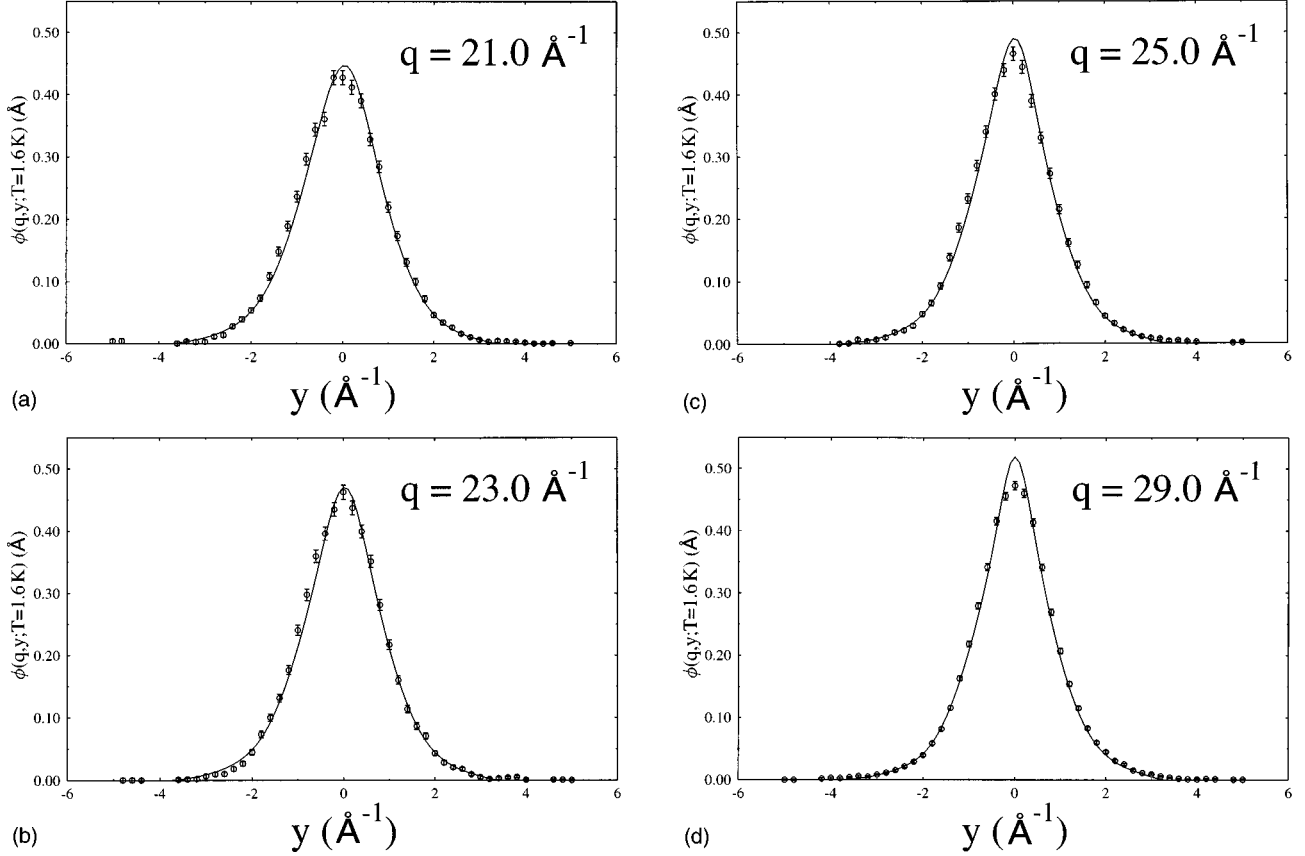


FIG. 2. (a)–(d) Same as Figs. 1(a)–1(d), for $T=1.6$ K, computed for $n_0(T=1.6 \text{ K})=0.087$.

Results for $R(q, y)$ for all cases discussed are assembled in Fig. 4 and show occasionally substantial differences. However, those are considerably smoothed by the single-particle momentum distribution [Eq. (5)] or density matrix in Eq. (6), and ultimately produce quite similar responses.^{4,9}

IV. CUMULANT EXPANSIONS OF THE RESPONSE

We consider below a method which has extensively been applied in the past³⁰ before the rediscovery of the $1/q$ GRS expansion of the response (4a).¹⁵ Recently it has been brought to the fore again in an attempt to parametrize data without the intervention of a theory. The method uses cumulant expansions of the Fourier transforms of the separate asymptotic and FSI parts of the response (5b), with coefficient functions related to moments of the response¹⁰

$$\tilde{\phi}(q, s) = \exp \left[\sum_{n \geq 2} \frac{(-is)^n}{n!} \bar{\mu}_n(q) \right], \quad (20a)$$

$$\tilde{F}_0(s) = \exp \left[\sum_{n \geq 2} \frac{(-is)^n}{n!} \bar{\alpha}_n \right], \quad (20b)$$

$$\tilde{R}(q, s) = \exp[\tilde{\Omega}(q, s)] = \exp \left[\sum_{n \geq 3} \frac{(-is)^n}{n!} \bar{\beta}_n(q) \right]. \quad (20c)$$

Using Eq. (5b) the various coefficient functions are related by $\bar{\mu}_n(q) = \bar{\alpha}_n + \bar{\beta}_n(q)$.³¹ Data for the response ϕ_E^{exp} are then compared with the parametrization (20)

$$\phi_E^{\text{exp}}(q, y) \Leftrightarrow \frac{1}{\pi} \text{Re} \int_0^\infty ds e^{iys} \tilde{\phi}_E(s, [\bar{\mu}_n(q)]), \quad (21)$$

where, as in Eq. (18) the right-hand side in Eq. (20a) includes ER. In principle, no *a priori* knowledge, or even meaning of the cumulant coefficient functions $\mu_n(q)$ is necessary for a search. However, it is natural to use motivated initial values, such as calculated ones.

Consider the normal fluid, in which case the q -independent cumulant coefficients $\bar{\alpha}_n$ originating in the asymptotic part of $\tilde{\phi}(q, s)$ can simply be expressed in terms of averages of even powers of the momentum of an atom, e.g.,

$$\bar{\alpha}_2 = \frac{1}{3} \langle p^2 \rangle,$$

$$\bar{\alpha}_4 = \frac{1}{5} \langle p^4 \rangle - \frac{1}{3} \langle p^2 \rangle^2, \text{ etc.} \quad (22)$$

The q -dependent coefficients $\bar{\beta}_n(q)$ relate to the FSI factors $\tilde{R}(q, s), \tilde{\Omega}(q, s)$ in Eq. (5b) and may be written as¹⁰

$$\begin{aligned} \bar{\beta}_n(q) &= \sum_{m=1}^{[(n-1)/2]} \left(\frac{1}{v_q} \right)^{n-2m} \bar{\beta}_{n,2m} \\ &= \sum_{m=1}^{[(n-1)/2]} \left(\frac{1}{q^*} \right)^{n-2m} z_{n,2m}. \end{aligned} \quad (23)$$

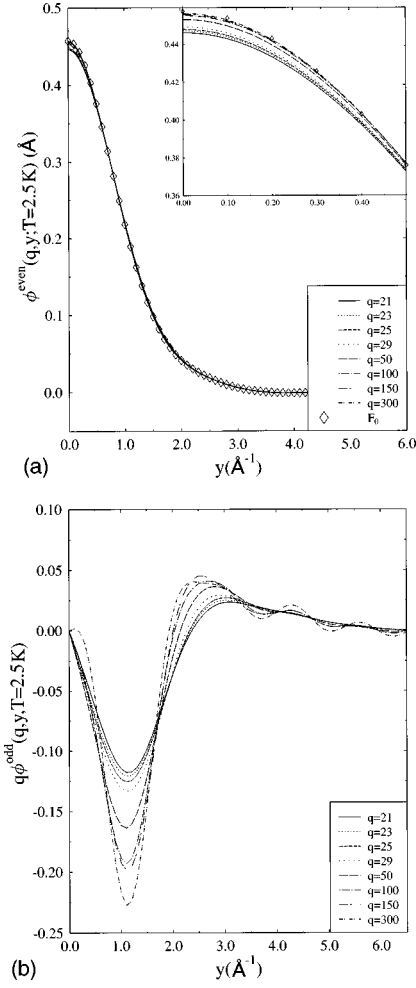


FIG. 3. (a) $\phi^{\text{even}}(q, y)$, part of the response even in y for $21 \leq q(\text{\AA}^{-1}) \leq 300$. For $q \geq 25 \text{\AA}^{-1}$ those cannot be distinguished from the asymptotic limit $F_0(y)$, Eq. (6). (b) $q\phi^{\text{odd}}(q, y)$, q times the response, odd in y for $21 \leq q(\text{\AA}^{-1}) \leq 300$.

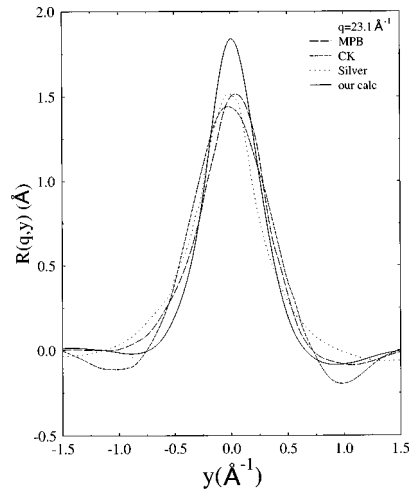


FIG. 4. FSI function $R(q=23 \text{\AA}^{-1}, y)$ in Eq. (5a), computed with the GRS choice for ρ_2 as well as for other descriptions. The drawn line is our result. Long dashes, short dashes, and dots are from Refs. 9, 8, and 5, respectively.

For convenience we use q^* , the momentum transfer parameter q in units of 10\AA^{-1} . Equation (23) displays q dependence and defines coefficients $z_{n,2m}$, which have the same dimensions and may be expressed in the same units as $\bar{\beta}_n$. The above are operators for dynamical variables of the system, averaged over *diagonal* l -body density matrices and their derivatives of order $l \leq n$. For the lowest-order cumulant coefficient functions one has

$$\bar{\beta}_3(q) = 6 \lim_{s \rightarrow 0} [\text{Im}\bar{\Omega}(q, s)/s^3] = 6 \lim_{s \rightarrow 0} [\text{Im}\bar{\Omega}_2(q, s)/s^3] \quad (24a)$$

$$= \frac{1}{6v_q} \langle \nabla^2 V \rangle_{\rho_2}, \quad (24b)$$

$$\bar{\beta}_4(q) = 24 \lim_{s \rightarrow 0} [\text{Re}\bar{\Omega}(q, s)/s^4], \quad (24c)$$

$$\bar{\beta}_5(q) = \frac{1}{v_q} \bar{\beta}_{54} + \left(\frac{1}{v_q}\right)^3 \bar{\beta}_{52}. \quad (24d)$$

Contrary to the GRS series in $1/q$, with coefficients depending on nearly-diagonal n -particle density matrices $\rho_n(\mathbf{r}_1 - s\hat{\mathbf{q}}, \mathbf{r}_2, \dots, \mathbf{r}_n; \mathbf{r}_1, \dots, \mathbf{r}_n)$, the moment approach underlying the cumulant expansion does not produce a systematic q dependence of the coefficient functions. For instance, *all* $\bar{\beta}_n(q)$ with odd n contain FSI contributions $\propto 1/q$. Equations (24a) and (24d) illustrate this for the dominant FSI coefficient functions $\bar{\beta}_n(q)$. Thus $\bar{\beta}_3(q) \propto 1/q$ draws exclusively on the BC contribution (7), while the two components of $\bar{\beta}_5$ are proportional to $1/q$ and $(1/q)^3$ due to binary, respectively, higher-order collision contributions, etc. It is the expansion of the semidiagonal $\rho_2(\mathbf{r}_1 - s\hat{\mathbf{q}}, \mathbf{r}_j; \mathbf{r}_1, \mathbf{r}_j)$ in s which produces an infinite number of contributions $\bar{\beta}_{2n+1}(q)$, all of which have parts $\propto 1/q$ with coefficients depending on *diagonal* densities [cf. Eq. (24b)] and their derivatives.

We start with the threshold behavior of the FSI phase $\bar{\Omega}(q, s)$, Eqs. (7),(10), and in particular of its imaginary part which, according to Eq. (24a), produces the dominant FSI parameter $\bar{\beta}_3(q)$. We checked that, within a few percent $q\text{Im}\bar{\Omega}_2(q, s)$ is, out to $s \approx 0.8 \text{\AA}$, independent of q . In particular we could extract the theoretical threshold value $z_3 = q^* \bar{\beta}_3^{\Omega_2}(q) = 6q^* \lim_{s \rightarrow 0} [\text{Im}\bar{\Omega}_2(q, s)/s^3] = 0.555 \text{\AA}^{-3}$ which over the entire range $q \leq 300 \text{\AA}^{-1}$ is, to better than 1%, independent of q . For the above reason one cannot determine the next order odd- n coefficients z_5 with reasonable precision.

We return to Eq. (24b) which seems to provide an independent way to calculate $\bar{\beta}_3(q)$. However, one can actually derive it from Eq. (24a), using Eq. (7) for $\bar{\Omega}_2$ in either version (9) or (10) for the generalized eikonal phase $\bar{\omega}(q, s)$. It holds for arbitrary semidiagonal ρ_2 which exactly satisfies Eq. (8b).³³

Using the same $g(r)$ as in ζ_2^{GRS} Eq. (14) we compute $q^* \bar{\beta}_3^{\nabla^2 V}(q) = 0.56 \text{\AA}^{-3}$. The agreement between $q^* \bar{\beta}_3^{\nabla^2 V}$ and $q^* \bar{\beta}_3^{\Omega}$ is very good, especially in view of the sensitivity of $q^* \bar{\beta}_3^{\nabla^2 V}$ on the precise shape of $g(r)$ where the Laplacian

TABLE I. Cumulant coefficient functions from data at $T=2.3$ K. The second column gives theoretical values. The third column gives seven-parameter fits with prescribed q^* behavior from (renormalized) data. Column 4 give fits when $q^*\bar{\beta}_3(q)$ is fixed at its starting values. Column 5 are fits if in addition $q^{*2}\bar{\beta}_4(q)$ is fixed. In the last column are results by Glyde *et al.*, who fitted $\mu_n(q)$ from a large set of data for different q .

Cumulant coefficient	Computed starting values	Seven-parameter fit for prescribed q dependence	Six-parameter fit; fixed $q^*\bar{\beta}_3$	Five-parameter fit; fixed $q^*\bar{\beta}_3, q^{*2}\bar{\beta}_4$	Glyde <i>et al.</i> (Refs. 10,11)
$\bar{\alpha}_2(\text{\AA}^{-2})$	0.916	0.910	0.913	0.914	0.897
$\bar{\alpha}_4(\text{\AA}^{-4})$	0.470	0.553	0.594	0.781	0.46
$\bar{\alpha}_6(\text{\AA}^{-6})$	0.337	0.535	0.613	0.700	0.38
$q^*\bar{\beta}_3(\text{\AA}^{-3})$	0.555	0.237	0.555	0.555	0.33
$q^{*2}\bar{\beta}_4(\text{\AA}^{-4})$	-2.268	-0.698	-0.993	-2.268	0
$q^*\bar{\beta}_{54}(\text{\AA}^{-5})$	0	0.416	0.851	0.615	0
$q^{*3}\bar{\beta}_{52}(\text{\AA}^{-6})$	0	-0.152	1.32	3.23	0.201
$q^{*2}\bar{\beta}_{64}(\text{\AA}^{-6})$	≈ -31.0				1.539

of V is large. The extraordinary stability of the extracted $q^*\bar{\beta}_3^{\bar{\Omega}}$ confirms the numerical consistency of the calculation.

As has been mentioned before, all FSI functions have been assumed to be T independent and we have used values for $T=0$. In order to estimate the influence of the temperature we have also calculated $q^*\bar{\beta}_3^{\bar{\Omega}^2 V}$ using a $g(r)$ obtained with PIMC at $T=2.8$ K.¹³ The result $q^*\bar{\beta}_3^{\bar{\Omega}^2 V}(T=2.8 \text{ K}) = 0.47 \text{ \AA}^{-3}$ confirms its sensitivity on the precise shape of $g(r)$.

Regarding parameters of even order in n one finds from $\text{Re}\bar{\Omega}_2(q, s)$, Eq. (24c) for the leading coefficient $z_{42} = q^{*2}\bar{\beta}_4^{\Omega_2}(q) = -2.26 \text{ \AA}^{-4}$. The next-to-leading $z_{64} \approx q^{*2}\bar{\beta}_{64}(q) \approx -31 \text{ \AA}^{-6}$ has been estimated from $\text{Re}\bar{\Omega}_2(s, q)$ for $s \geq 0.1 \text{ \AA}$.

An important remark is in order here. While $\bar{\beta}_3$, the leading FSI coefficient of odd order, is entirely given by the BC approximation, the first nonvanishing, even order coefficient $\bar{\beta}_4$ has additional contributions from higher-order FSI. Direct evidence for their existence is provided by the exact expression $\bar{\beta}_4 \propto \langle (\nabla V)^2 \rangle$, i.e., the average of the squared force on the struck atom. The latter is positive definite^{10,34} whereas in the above-mentioned BC approximation $\bar{\beta}_4^{\Omega_2} < 0$. We recall that the latter derives from $\text{Re}\bar{\Omega}_2$, with $\text{Re}\bar{\Omega}_2 \ll \text{Im}\bar{\Omega}_2$. It is therefore plausible that higher-order FSI contributions overwhelm the small BC part, leading to an overall positive $\bar{\beta}_4$.

At this point we recall the comment in the Introduction on FSI parameters, based on the outcome of the cumulant analysis by Glyde *et al.*^{10,11} At first sight the misfit of, specifically $\bar{\beta}_3$, may conceivably affect the parameters for the momentum distribution and, if true, put in question a successful determination of $n(p)$. This was the main reason why we wanted to repeat the analysis.

We report below several results for fits of cumulant parameters to the experimental response (21). Those have been obtained with the CERN MINUIT code, as applied to the ten $T=2.3$ K data sets in the range $21 \leq q(\text{\AA}^{-1}) \leq 29$ from Azuah's thesis.³ We first note that the integrated strengths of

the data there appear for all q to be approximately 1.4% in excess of the exact result 1. By construction that demand is exactly fulfilled by a cumulant expansion (20a) in, no matter what approximation. We also considered data, cut at $y \approx 3.0-3.4 \text{ \AA}^{-1}$ where statistical noise in very small responses, may cause those to have negative values. The latter appear to hardly affect the extracted parameters.

The above source of information does not contain numerical data and ER for the lower q data. As a consequence we had to limit ourselves to a small data base which is bound to influence the FSI parameter functions which increases with decreasing q .

Our results for $T=2.3$ K are assembled in Table I. We entered in column 2 theoretical values for the parameters, calculated as indicated in Eq. (24), or set to 0 when impossible to evaluate reliably. Notice that the negative z_6 , obtained from a limited s range, will generate an unbounded $\bar{R}(q, s)$, barring a convergent Fourier transform of $\bar{R}(q, s)$. Actually we did not consider z_6 in the fits and restrict ourselves to a maximum of seven parameters as discussed below.

Column 3 is the result of a seven-parameter fit for cumulant coefficients functions with theoretical q dependence and encompasses therefore all ten data sets in our q range. Columns 4 and 5 are six-, respectively, five-parameter fits like in column 3, when first $q^*\bar{\beta}_3(q)$ alone and then also $q^{*2}\bar{\beta}_4(q)$ are held at their theoretical values.

Notice, that not only the extracted $\bar{\beta}_4^{\Omega_2}$ [Eq. (24c)] in the BC approximation, but also fitted values are negative, at least when higher-order even coefficients in the cumulant series are neglected. This can be understood if one tries to fit the data for all q using a polynomial in s with a finite number of $\bar{\beta}_n(q)$ as coefficients. However, those no more reproduce the low- s behavior of the FSI phase $\bar{\Omega}(q, s)$. It is also clear that a fit is only possible if $\lim_{|s| \rightarrow \infty} \bar{R}(q, s) \rightarrow 0$. For an expansion up to $n=4$ this implies a negative $\bar{\beta}_4(q)$.

We now reach the extraction of $\bar{\mu}_n(q)$ for each q and the *determination*, as opposed to the above *assumption*, of their q dependence. This appeared to be impossible for the limited

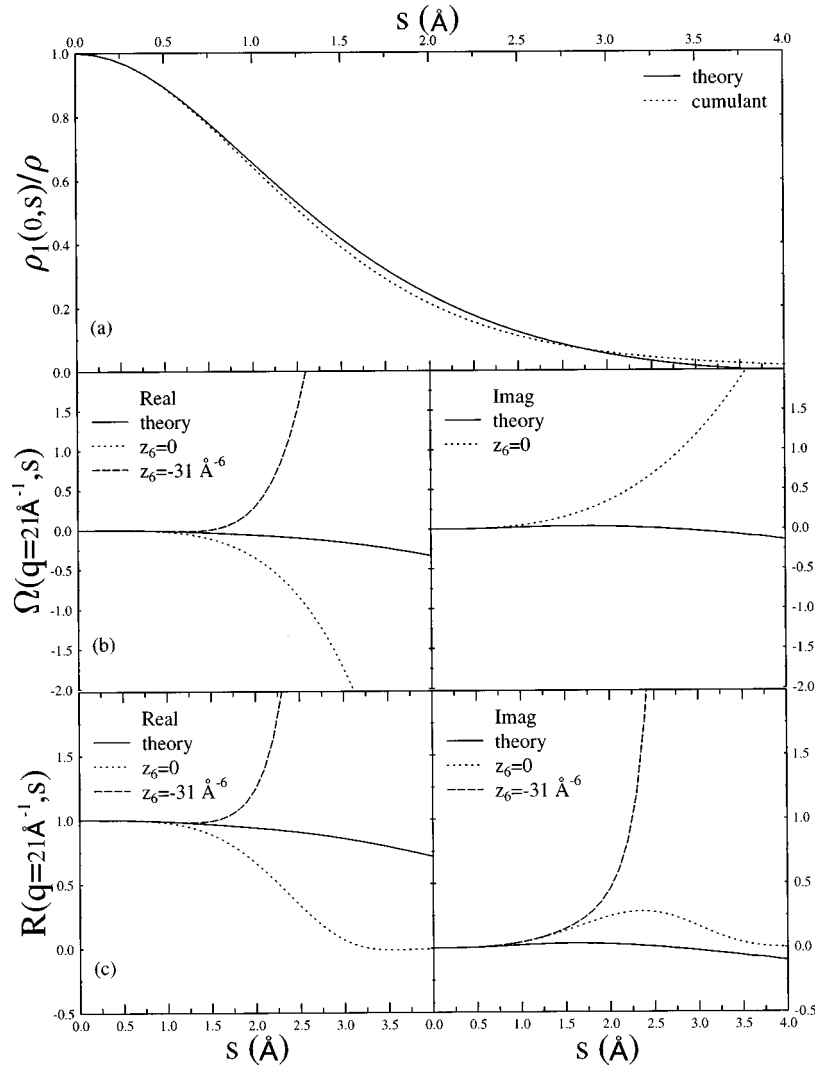


FIG. 5. (a) Comparison of the single atom density matrix $\rho_1(0,s)/\rho$ and its sixth-order cumulant expansion. (b) Real and imaginary parts of the BC FSI phase $\tilde{\Omega}_2(q,s)$ ($q=21 \text{ \AA}^{-1}$) from theory and represented by a fifth-, respectively, sixth-order cumulant expansion; (c) the same for the FSI factor $\tilde{R}(q,s)$.

data set available to us. However, Glyde *et al.* had access to far more data and we enter their results in the last column taken from Table I of Ref. 11. As the reported z_4 is zero, a positive value of z_6 is required to give a convergent Fourier transform of $\tilde{R}(q,s)$.

First we remark that the parameters, resulting from the fits from columns 3–6, all produce good fits to the response data. However, those fits do not resolve the disagreement between theoretical and extracted FSI parameters. Table I shows even smaller values for $z_3=q^*\beta_3(q)$ than reported in Refs. 10,11.

In fact, we find the results of column 5 in Table I most telling. Fixing the dominant FSI parameters $z_{3,4}$ at their theoretical values, one expects $\bar{\alpha}_4, \bar{\alpha}_6$ to settle close to their starting values. This appears not to be the case: Column 5 appears to produce the poorest agreement between any of the reconstructed and the computed $n(p)$ (see Fig. 6 below).

To understand the above, we turn again to the calculated $\tilde{\Omega}(q,s)$ which we recall, produces very good fits to the data (Figs. 1,2). Although not called for in calculations using a dynamic theory, Eqs. (5b) and (20c) show that the expansion

of $\tilde{\Omega}(q,s)$ in s produces, in principle, the cumulant coefficients and in particular the FSI parameters $\bar{\beta}_n(q)$.

The complete cumulant series is of course equivalent to the exact $\tilde{\Omega}$, but a truncation at some n obviously reproduces behavior up to some relatively low s . The crucial question is to what order one should go, and the answer clearly depends on the effective s range of each of the component factors. Those are according to Eqs. (5b), (18), and (21) the single-atom density distribution $\rho_1(0,s)/\rho$, the FSI interaction factor $\tilde{R}(q,s)$ [or $\tilde{\Omega}(q,s)$], and the Fourier transform $\tilde{E}(q,s)$ of the ER function.

Next, we report on tests where we compare not data, but theoretical values of the input factors $\rho_1(0,s), \tilde{R}, \tilde{\Omega}$ and their cumulant approximations $\tilde{R}^{cu,n}, \tilde{\Omega}^{cu,n}$ to order n . The coefficients defining $\tilde{R}^{cu,n}, \tilde{\Omega}^{cu,n}$ are given in column 2 of Table I. Figure 5(a) shows over the relevant s range reasonable adequacy of the cumulant expansion for $\rho_1(0,s)/\rho$ to order $n=6$. Next, Figs. 5(b), 5(c) give Re and Im parts of $\tilde{\Omega}(q,s)$, respectively, $\tilde{R}(q,s)$ $q=23 \text{ \AA}^{-1}$ and shows that the FSI cu-

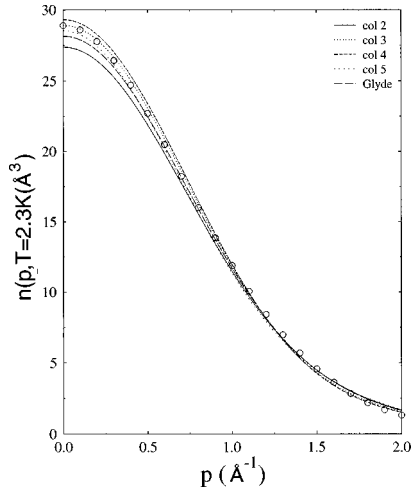


FIG. 6. The single atom momentum distribution for $T=2.3$ K, reconstructed from the various cumulant fits, assembled in Table I, including the one from theoretical starting values. The curves, labeled c_n correspond to increasing column number in Table I, including the fit by Glyde *et al.* (Glyde). The circles are values calculated in Ref. 13.

mulant series, truncated at $n=5$, rapidly falls short of the computed functions for $s \geq 1 \text{ \AA}^{-1}$. Inclusion of the above-mentioned, well-determined $z_6 \approx z_{64}$ affects only $\text{Re}\tilde{\Omega}$ [cf. Eq. (20b)]. It extends the agreement between the calculated and cumulant expansions for the two FSI functions over a modest additional s range, but does not prevent rapid deterioration of $\tilde{R}(q,s), \tilde{\Omega}(q,s)$ from 1.2 \AA^{-1} on. As mentioned before the estimated z_6 gives rise to a nonbound $\tilde{R}(q,s)$. Since terms in the cumulant expansions (24) in powers of s have alternating signs, the order of β_n to be retained depends on the s range one wishes, or needs to cover.

The given observations do not contradict the high-quality reproduction of the response data, when generated by a best fit of the parameters in a polynomial representation of $\tilde{\Omega}(q,s)$, Eq. (24c), to the data. However, the parameters obtained in this way differ considerably from the expansion coefficients in s of the FSI phase $\tilde{\Omega}(q,s)$. As has been mentioned above, the failure is due to the insufficiency of finite order cumulant representations $\tilde{R}^{cu,n}, \tilde{\Omega}^{cu,n}$ and will only disappear if for sufficiently high n , FSI functions will coincide with their cumulant expansion out to the relevant medium s .

The above is, in our opinion, the source of the discrepancy between calculated and extracted FSI parameters. In spite of correlations between fitted parameters, there is sufficient meaning to the extracted FSI to justify the above conclusion. Were it not for the overwhelming role of the asymptotic part and its representation by a truncated cumulant series, one could not trust the extracted $\bar{\alpha}_n$.

The sensitivity of the fitting procedure can be judged from Fig. 6, where we reconstruct single-atom momentum distributions from the various fits for α_n . Dense dots, short dashes, and spaced dots are results using columns 3–5 from Table I. Long dashes are from the last column, i.e., the fit of Glyde *et al.*, while the drawn line corresponds to the theoretical cumulant parameters in column 2. We recall that the

α parameters in that column are based on the computed distribution $n(p, T=2.5 \text{ K})$,¹³ marked by circles. The nevertheless imperfect fit for the reconstructed $n(p)$ is again due to the finite-order expansion of $\rho_1(0,s)$ causing a moderate misfit for large s . Otherwise all reconstructed distributions are of comparable quality: $n(p)$ is clearly well determined by the data.

V. SUMMARY AND CONCLUSIONS

We addressed above three topics regarding the response of liquid ^4He , retrieved from the inclusive scattering of neutrons. Using dynamics we first made predictions for the recent MARI data, taken at temperatures both below and above T_c . We analyzed the range of momentum transfers $21 \leq q(\text{\AA}^{-1}) \leq 29$, for which we had available data and experimental resolution and obtained good agreement with experiment.

A second topic was the approach of the response to its asymptotic limit in q for fixed scaling variable y . For smooth interactions between constituents, that approach is rigorously $\propto 1/q$, but the same is not guaranteed when a strong short-range repulsion is present in the atom-atom interaction V . We investigated theoretically the response for $q \leq 300 \text{ \AA}^{-1}$ for the actual V with its short-range repulsion, and what we found reconfirmed our findings from a few years ago based on medium- q data: final-state-interaction contributions, over and above the asymptotic part, still decrease approximately as $1/q$.

Regarding the q values for which the response has been measured, we repeat what was already evident from the older data:⁴ there is no additional information to be retrieved by increasing q by less than 20–30 % and no new information at all at very high q .

Our last topic was a refit of the expansion coefficient functions, which parametrize data. A previous analysis led to a single-atom momentum distribution in good agreement with computed $n(p, T)$, but did not produce the main FSI coefficient function. Its influence in the large- q region is too marginal to be extracted from the data with present accuracies. This does not change our judgment that little can be added to *understanding* the data on the response of liquid ^4He at high momentum.

In spite of minor discrepancies, a summary of the treatment of the first two topics is definitely positive. Presumably for no atomic, molecular, nuclear or subnuclear system for which the response has been measured, has one reached asymptotia as clearly and as well understood as for liquid ^4He . Of course, asymptotia is not simply the mathematical limit $q \rightarrow \infty$ for fixed y . Increasing q requires increasing beam energy, ultimately beyond the ionization energy $\approx 39 \text{ eV}$. A description of the response then requires the inclusion of additional electronic degrees of freedom to translational ones.

Finally we venture an outlook for future explorations of inclusive scattering which almost certainly implies extension of experiments to larger momentum transfers q . Our judgement is based on Eqs. (5b) and (7). In that representation for the response, the FSI factor $\tilde{R}(q,s)$ does not depend on the

single-particle density $\rho_1(0,s)$ and in particular not on the condensate fraction for $T \leq T_c$. Together with Eq. (19) this implies the universality of the asymptotic limit (4b) under all circumstances. One then tends to believe that present experiments and theory seem to have exhausted the search for information contained in the response of liquid ^4He at high momentum.

ACKNOWLEDGMENTS

A.S.R. thanks the Department d'Estructura e Constituents de la Materia, Universitat De Barcelona for hospitality and support. The authors are indebted to H. Glyde for correspondence and discussions. They are also grateful to D. Ceperley for supplying $g(r)$ at finite temperatures. This work was partially supported by DGICYT (Spain) Grant No. PB95-0761.

- ¹H. R. Glyde, *Excitations in Liquid and Solid He* (Oxford University Press, Oxford, 1994).
- ²K. H. Andersen *et al.*, *Physica B* **180/181**, 865 (1992); **197**, 198 (1994).
- ³R. T. Azuah, Ph.D. thesis, University of Keele, 1994.
- ⁴T. R. Sosnick, W. M. Snow, and P. E. Sokol, *Phys. Rev. B* **41**, 11 185 (1990); T. R. Sosnick, W. M. Snow, R. N. Silver, and P. E. Sokol, *ibid.* **43**, 216 (1990).
- ⁵R. N. Silver, *Phys. Rev. B* **37**, 3794 (1988); **38**, 2283 (1988); **39**, 4022 (1989).
- ⁶A. S. Rinat and M. F. Taragin, *Phys. Rev. B* **41**, 4247 (1990).
- ⁷A. S. Rinat, *Phys. Rev. B* **42**, 9944 (1990).
- ⁸C. Carraro and S. E. Koonin, *Phys. Rev. B* **41**, 6741 (1990); *Phys. Rev. Lett.* **65**, 2792 (1990).
- ⁹F. Mazzanti, J. Boronat, and A. Polls, *Phys. Rev. B* **53**, 5661 (1996).
- ¹⁰H. R. Glyde, *Phys. Rev. B* **50**, 6726 (1994).
- ¹¹H. R. Glyde, R. T. Azuah, K. H. Anderson, and W. G. Stirling (unpublished); R. T. Azuah, W. G. Stirling, H. R. Glyde, P. E. Sokol, and S. M. Bennington, *Phys. Rev. B* **51**, 605 (1995).
- ¹²K. H. Andersen, W. G. Stirling, and H. R. Glyde, *Phys. Rev. B* **56**, 8978 (1997).
- ¹³D. M. Ceperley and E. L. Pollock, *Can. J. Phys.* **65**, 1416 (1987); (private communication).
- ¹⁴P. A. Whitlock and R. M. Panoff, *Can. J. Phys.* **65**, 1409 (1987).
- ¹⁵H. A. Gersch, L. J. Rodriguez, and Phil N. Smith, *Phys. Rev. A* **5**, 1547 (1973).
- ¹⁶G. B. West, *Phys. Rep.*, *Phys. Lett.* **18C**, 264 (1975).
- ¹⁷H. A. Gersch and L. J. Rodriguez, *Phys. Rev. A* **8**, 905 (1973).
- ¹⁸J. Besprosvany, *Phys. Rev. B* **43**, 10 070 (1991).
- ¹⁹A. S. Rinat and M. F. Taragin, *Phys. Lett. B* **267**, 447 (1991).
- ²⁰C. Carraro and A. S. Rinat, *Phys. Rev. B* **45**, 2945 (1992).
- ²¹A. S. Rinat and M. F. Taragin, *Nucl. Phys. A* **598**, 349 (1996).
- ²²R. A. Aziz, V. P. S. Nain, J. S. Carley, W. L. Taylor, and J. T. McConville, *J. Chem. Phys.* **70**, 4330 (1979).
- ²³One knows more details of the shape of the momentum distribution of the condensate fraction (Ref. 24) than is implicit in Eq. (12), but the latter suffices for our limited purposes below.
- ²⁴J. Gavoret and P. Nozieres, *Ann. Phys. (N.Y.)* **28**, 349 (1964).
- ²⁵D. M. Ceperley, in *Momentum Distributions*, edited by R. N. Silver and P. E. Sokol (Plenum, New York, 1989), p. 71.
- ²⁶M. L. Ristig and J. W. Clark, *Phys. Rev. B* **40**, 4355 (1989).
- ²⁷Q. N. Usmani, B. Friedman, and V. R. Pandharipande, *Phys. Rev. B* **25**, 4502 (1982).
- ²⁸A. S. Rinat, *Phys. Rev. B* **40**, 6625 (1990).
- ²⁹E. C. Svenson, V. F. Sears, A. D. B. Woods, and P. Martel, *Phys. Rev. B* **21**, 3638 (1981).
- ³⁰V. F. Sears, *Phys. Rev. B* **30**, 44 (1984), and references contained therein.
- ³¹The quest for manageable magnitudes for the coefficients $\bar{\alpha}_n, \bar{\beta}_n(q), \bar{\mu}_n(q)$ which have dimensions l^{-n} , has occasionally led to the introduction of artificial combinations of units which varied with the order n (Refs. 10,11). A possible candidate for such a length is the mean free path of an atom in the medium. From measured, weakly oscillating total atom-atom cross sections in the relevant q range (Ref. 32), one estimates $2\lambda = [\rho\sigma_q^{\text{tot}}/2]^{-1} \approx 1.6 \text{ \AA}$, which may serve as a scale for the recoil length s . For instance, Eq. (20a) would become
- $$\bar{\phi}(q,s) = \exp\left[\sum_{n \geq 2} \frac{(-is)^n}{n!} \bar{\mu}_n(q)\right] = \exp\left[\sum_{n \geq 2} (-is/2\lambda)^n M_n(q)\right],$$
- with the now dimensionless $M_n(q) = (2\lambda)^n \bar{\mu}_n(q)/n!$. The thus defined coefficients permit an estimate of their relative size.
- ³²R. Feltgen, H. Pauly, F. Torello, and H. Veymeyer, *Phys. Rev. Lett.* **30**, 820 (1973); R. Feltgen, H. Kirst, K. A. Koehler, H. Pauly, and F. Torello, *J. Chem. Phys.* **76**, 2360 (1982).
- ³³The above seems to run counter to a statement by Glyde [text after Eqs. (19,28) in Ref. 1, p. 340] that evaluations starting from Eq. (5b) forcibly lead to a factor -2 difference between Eqs. (24a) and (24b). The latter is easily shown to be caused by the use of a diagonal instead of a semidiagonal ρ_2 in $\tilde{\Omega}_2$. [The semiclassical approximation (12) is not exactly in that category and for it, the right-hand side of Eq. (24b) has to be supplemented by a small correction of relative order $\mathcal{O}(q^{-2})$].
- ³⁴A. Rahman, K. S. Singwi, and A. Sjölander, *Phys. Rev.* **126**, 986 (1962).